Climate Dynamics (2004) 22: 771–781
DOI 10.1007/s00382-004-0416-y

Z. Liu · W. Lewis · A. Ganopolski

An acceleration scheme for the simulation of long term climate evolution

Received: 28 October 2002 / Accepted: 11 February 2004 / Published online: 30 April 2004

Abstract An acceleration scheme is proposed in a coupled ocean-atmosphere model for the simulation of long term climate evolutions forced by climate forcing of longer than millennia time scales. In this "coordinated acceleration" scheme, both the surface forcing and the deep ocean are accelerated simultaneously by the same factor. The acceleration scheme is evaluated in a 3-dimensional ocean general circulation model and in a coupled ocean-atmosphere model of intermediate complexity. For millennial climate evolution, our acceleration scheme produces reasonably good simulations with an acceleration factor of about 5. For climate evolution of even longer time scales, the acceleration factor can be increased further.

1 Introduction

Climate evolution on millennia and longer time scales is important for our understanding of global climate changes in the past and future. One example is the climate evolution since the Last Glacial Maximum (LGM) (21 000 years ago). In the context of a coupled ocean-atmosphere model, this 20 000-year long climate evolution is forced predominantly by the slow change of orbital forcing, glacial boundary condition and atmospheric greenhouse gases. At present, this type of long-term climate simulation remains as a great computational challenge in a fully coupled ocean-atmosphere general circulation model (OAGCM).

Z. Liu (✉) · W. Lewis
Center for Climatic Research, and Department of Atmospheric of Oceanic Science, University of Wisconsin-Madison, USA
E-mail: zliu3@facstaff.wisc.edu

Z. Liu
1225 W. Dayton St., Madison, WI 53706-1695, USA

A. Ganopolski
Potsdam Institute for Climate Impact Research,
Potsdam, Germany

Two types of acceleration schemes have been proposed for an OAGCM, the asynchronous coupling (Manabe and Bryan 1969; Suasen and Voss 1996; Liu et al. 1999), and the periodically synchronous coupling (proposed by Gates, see Schlesinger 1979; Sausen and Voss 1996; Voss and Sausen 1996; Voss et al. 1998). In the former, the atmosphere-alone model and ocean-alone model are integrated alternatively, while in the latter, the coupled model and the ocean-alone model are integrated alternatively. In both schemes, the reduction of computation time is achieved in the periods of the ocean-alone integration, with the integration time shorter than that in the synchronously coupled simulation. As a result, in both schemes, the computation time is reduced only for the atmosphere model, not for the ocean model. These schemes therefore are of limited value to very long OAGCM simulations that also require substantial computation of the ocean component model. Taking advantage that the computation of the ocean model is limited mainly by the faster upper ocean circulation, Bryan (1984) proposed a general deep water acceleration scheme that saves computation time for the ocean model. The reduction of computational time is now achieved by the acceleration of the deep ocean. This general deep water acceleration scheme, however, has so far been used mainly for simulations of the OAGCM under equilibrium climate forcing, such as the spin-up stage of an OAGCM.

Here, we propose a new acceleration scheme which is partly based on the idea of deep water acceleration. In our scheme, both the deep water and the surface forcing are accelerated by the same factor simultaneously. This scheme will be called the "coordinated" acceleration scheme, because of the required precise coordination between the accelerations of both the climate forcing and the deep ocean. This scheme reduces the computation time for both the atmosphere and ocean. However, this scheme is valid only for long-term climate evolutions forced by slowly varying climate forcing of time scales comparable or longer than that of the deep ocean circulation. Our sensitivity study suggests that this scheme can achieve an acceleration of about five times for millennial climate evolution, and even higher acceleration for even longer climate evolution. The basic idea of the acceleration scheme is discussed in Sect. 2. The performance of the acceleration scheme is evaluated in a 3-dimensional OGCM in Sect. 3 and in a coupled climate model of intermediate complexity in Sect. 4. The conclusion and further discussions are given in Sect. 5.

2 The principle of coordinated acceleration

The basic idea of the acceleration can be described, schematically, in a coupled model of the form

$$\begin{aligned} &\frac{\partial}{\partial t}T_a = A(T_a, T_{o1}, T_{o2}, \ldots T_{oN}) + F(t), \\ &\frac{\partial}{\partial t}T_{on} = O_n(T_a, T_{o1}, T_{o2}, \ldots T_{oN}), \quad n = 1, 2, \ldots .N \ , \end{aligned} \tag{1}$$

where T_a is the atmosphere temperature, T_{on} is the ocean temperature at level n, A and O_n are functions of T_a, T_{on} and their spatial derivatives, and $F(t)$ is a transient climate forcing anomaly. The system is integrated to the characteristic time scale of the climate forcing t_{End}, such that Eq. (1) is valid in

$$0<t \leq t_{End} \ . \tag{2}$$

Without loss of generality, we also assume that the maximum time step for numerical stability is Δt_M, such that a finite-difference form of Eq. (1) is numerically stable only for

$$\Delta t<\Delta t_M \ . \tag{3}$$

To reduce the integration time, the entire system Eqs. (1,2) can be accelerated by a factor $C(>1)$ such that

$$\begin{aligned} &\frac{1}{C}\frac{\partial}{\partial t}T_a = A(T_a, T_{o1}, T_{o2}, \ldots T_{oN}) + F(Ct), \\ &\frac{1}{C}\frac{\partial}{\partial t}T_{on} = O_n(T_a, T_{o1}, T_{o2}, \ldots T_{oN}), \quad n = 1, 2, \ldots N \ , \end{aligned} \tag{4}$$

$$0<t \leq t_{End}/C \ . \tag{5}$$

The identity of the system Eqs. (1,2) and (4,5) is obvious with the transformation of a fast time variable

$$\tau = Ct \tag{6}$$

in Eqs. (4,5). The system Eqs. (4,5) will be called a completely accelerated system, in which the integration time is reduced by the acceleration factor C. In practice, however, this shorter integration time does not gain us any computational efficiency, because the time step has to be reduced by the same factor C to satisfy numerical stability. This follows because the time step for the finite difference form of Eq. (4) needs to satisfy

$$\Delta t<\Delta t_M/C \ . \tag{7}$$

Nevertheless, this completely accelerated system can be modified. First, as noted by Bryan (1984), the numerical stability criterion Eq. (5) is usually limited by the faster components of the coupled system: the atmosphere T_a and the upper ocean T_{on}, say, of $1 \leq n \leq N_1$. Second, physically, we are interested in the forced climate response to a slow forcing that has a time scale much longer than that of these faster components. At the slow forcing time scales, therefore, the statistical annual climate state of these faster components will be in a quasi-equilibrium balance.

$$\begin{aligned} &0 \approx A(T_a, T_{o1}, T_{o2}, \ldots T_{oN}) + F(Ct), \\ &0 \approx O_n(T_a, T_{o1}, T_{o2}, \ldots T_{oN}), \quad n \leq N_1 \ . \end{aligned} \tag{8}$$

With this balance, the solution will remain little changed for any acceleration factor on these layers (as long as it is not too large to slow down the faster variability to be comparable with the slow forcing time scale). Indeed, were Eq. (8) exact, it would remain so no matter what a constant is multiplied. With these two points in mind, we propose a partially accelerated scheme, in which both the surface forcing and deep ocean are accelerated simultaneously by a same factor C, while leaving the atmosphere and upper ocean not accelerated. That is:

$$\begin{aligned} &\frac{\partial}{\partial t}T_a = A(T_a, T_{o1}, T_{o2}, \ldots T_{oN}) + F(Ct), \\ &\frac{\partial}{\partial t}T_{o1} = A(T_a, T_{o1}, T_{o2}, \ldots T_{oN}), \quad 1 \leq n \leq N_1 \\ &\frac{1}{C}\frac{\partial}{\partial t}T_{on} = O_n(T_a, T_{o1}, T_{o2}, \ldots T_{oN}), \quad N_1<n \leq N \ . \end{aligned} \tag{9}$$

The integration time now remains the same as in Eq. (5)

$$0<t \leq t_{End}/C \ . \tag{10}$$

This partial acceleration system Eqs. (9,10), will be called the coordinated acceleration system because of the coordinated acceleration of the same factor in both the forcing and the deep ocean. This scheme maintains the short integration time of the complete acceleration system Eqs. (4,5) as well as the numerical stability criterion (3) of the original system Eqs. (1,2). The latter is true because the numerical stability criterion is determined by the faster components only, which are not accelerated here. Thus, the partial acceleration system (9, 10) accelerates the original system (1, 2) effectively by a factor of C.

The general idea of the coordinated acceleration above has been tested successful in a zero-dimension energy balance model similar to that of Suasen and Voss (1996, not shown). However, for this scheme to be of practical value, more realistic models are needed to quantify the performance of the scheme. How much is the error of the acceleration scheme? Under what conditions is the acceleration scheme most efficient? These questions can be answered only after a through evaluation of a realistic global model whose ocean memory is simulated with reasonable accuracy at different depths. An OAGCM is ideal, but impractical because of the limitation of computational resources. Considering the most critical role of a realistic ocean memory here, we will first evaluate the acceleration scheme in an OGCM.

3 Application to an OGCM

3.1 An example

We used the GFDL-MOM3.0 (Pacanowski and Griffies 1998) with a realistic world ocean domain and bottom topography. The model has a resolution of 4° lat. × 4° long. × 15 levels and is integrated with a time step of 1 day for the temperature and salinity equations, and 1 h for the momentum equations. The model is first spun-up to a steady state for 5000 years using the seasonal cycle of the observed wind stress, SST and SSS. The SST and SSS are restored towards the Levitus SST and SSS respectively, with a restoring time of 30 days for the top layer of 30 m. A transient anomalous climate forcing is then imposed with a globally uniform restoring SST that increases linearly from 0 °C at year 0 to 2 °C at the end of the forcing period.

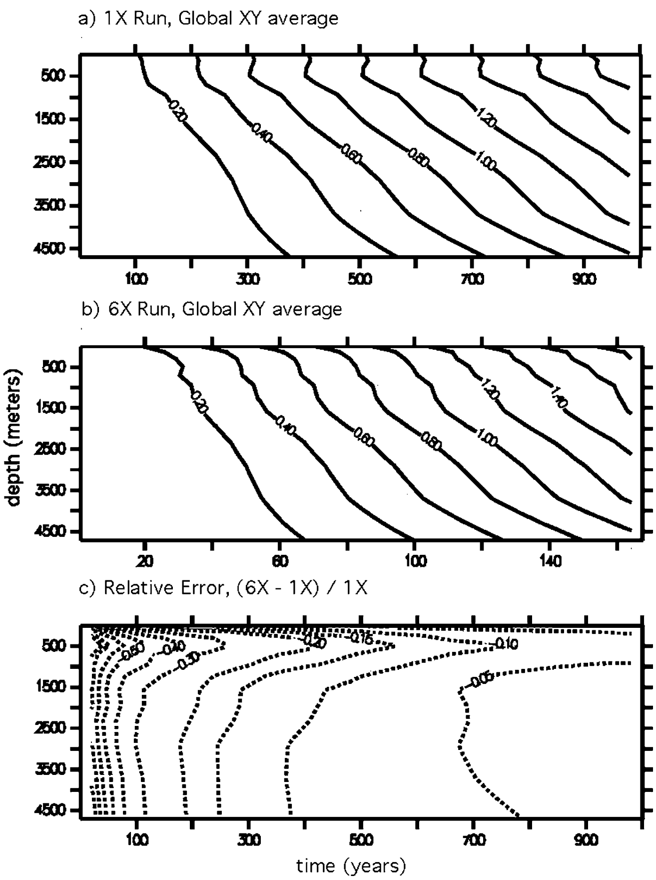

Fig. 1a–c Time-depth plot for the evolution of global mean temperature changes in response to a global SST anomaly forcing that increases from 0 to 2 °C in 1000 years. Temperature anomaly is shown in **a** for the 1X run (without acceleration) and in **b** for the 6X run. The relative error, as defined in Eq. (11), is shown in **c**. The vertical profile for the ocean acceleration is the profile *B* in Fig. 3b

Figure 1 shows an example under a SST forcing of 1000 years. For the synchronous simulation ($C = 1$, 1X run) (Fig. 1a), the time evolution of the global average temperature anomaly (Fig. 1a) shows a gradual downward penetration of the surface warming (Fig. 1a). At year 1000, the water column is still undergoing an apparent transient warming, with a "final" warming about 2 °C at the surface and 1 °C at the bottom. It should be noted however, that this "final" warming is not the equilibrium response, because a transient forcing has been applied.

A coordinated acceleration scheme is then applied with the surface forcing accelerated by 6 times ($C = 6$, 6X run). In the ocean, the tracer equations have an acceleration factor that is 1 in the upper 500 m and that increases linearly to 6 at 700 m and remains at 6 below 700 m. No acceleration is applied to the momentum equations, as in Bryan (1984). The model is integrated for 1000 years/6 = 166 years. The most striking feature is a surprising similarity of the global temperature evolution between the 6X run (Fig. 1b) and the synchronous 1X run (Fig. 1a). For example, both have a final warming 2 °C at the surface and 1 °C at the bottom.

The accuracy of the 6X run is further assessed by comparing the 6X run and the 1X run of the corresponding years. At year n, the absolute and relative errors are defined as

$$AE = T_{1X}|_{t=n} - T_{6X}|_{t=n/C} \ , \tag{11}$$

$$RE = AE/T_{1X}|_{t=n} \ . \tag{12}$$

The temporal evolution of the relative error of the 6X run is shown in Fig. 1c. The most important feature is a small final relative error: less than 5% over most of the water column and with the maximum of less than 10%. The similarity between the two runs can also be seen in the final zonal mean ocean temperature changes (Fig. 2). A comparison of the 1X (Fig. 2a) and 6X (Fig. 2b) runs shows a striking similarity, especially in the deep ocean. For example, both runs show a strong warm tongue penetrating from the surface downward at higher latitudes in each hemisphere, with the Southern Ocean tongue deeper and stronger. Both have the minimum warming response at the northern abyssal ocean at about *33*°N. Some features in the upper ocean are also well simulated, such as the maximum warming centered at 40°S and 500 m, and the minimum warming centered at 45°N and 1000 m. The relative error (Fig. 2c) is generally smaller than 5% over the entire ocean, except for the upper 1000 m. Overall, the 6X run reproduces the 1X simulation surprisingly well. This example demonstrates the feasibility of the coordinated acceleration, at least for the 1000-year climate evolution here.

The 6X run also has a persistent negative error, with its maximum at the intermediate level around the depth

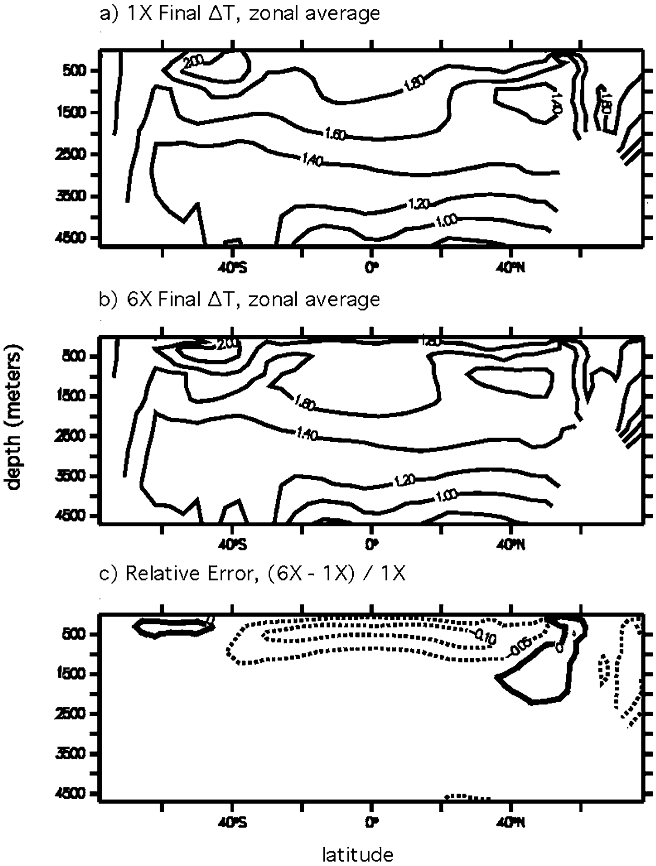

Fig. 2 Meridional sections of the final changes of the zonal mean global ocean temperatures for **a** the 1X run at year 1000, **b** the 6X run at year 166 year, and **c** the relative error of the 6X run. The two experiments are the same as those in Fig. 1

of 500 m (Fig. 1c) and in the mid- and low- latitudes (Fig. 2c). This error structure can be understood as follows. The SST has a very fast time scale because it is now directly forced by the surface restoring SST forcing with a short restoring time. The SST is therefore virtually in equilibrium with the forcing as in Eq. (8) and therefore has little error. Towards the subsurface, the oceanic memory increases because of the finite heat storage term $\partial_t T$, and the quasi-equilibrium balance Eq. (8) becomes less accurate. The finite heat storage time tends to delay the upper ocean warming. Since the ocean just below 500-m is accelerated less than the surface forcing, the finite ocean delay results in a persistent negative error in the 6X run. This upper ocean delay can be seen by comparing the 1X run in Fig. 1a and the 6X run in Fig. 1b: the surface warming penetrates quickly downward to 500 m (with vertical isotherms) in the former, but penetrates gradually downward (with tilted isotherms) in the latter. This delay error is the largest in the mid- to low-latitude upper ocean (Fig. 2c), where the oceanic surface signals are ventilated downward slowly at decadal time scales (Luyten et al. 1983). Deeper still the relative error decreases because the ocean is accelerated the same as the surface forcing. This perfect acceleration match in the deep ocean should generate no error, were the upper stream condition (upper ocean) correct. However, as discussed, the upper ocean condition is delayed. Therefore, the deep ocean also exhibits a delayed response but with a smaller magnitude.

3.2 Dependence of the time scale of forcing

An important feature of the coordinated acceleration scheme is that its accuracy increases with the time scale of the forcing. This follows from our basic idea in Sect. 2: a longer time scale is better represented by the quasi-equilibrium of the upper ocean Eq. (8), and a smaller acceleration factor distorts less the true simulation. This time-scale dependency is implied in Fig. 1c. It is seen that the relative error decreases with time (Fig. 1c). (The large relative error in the initial stage is caused by a small absolute signal (Fig. 1a), rather than a large absolute error.) Assuming an approximately linear ocean response to surface forcing, the large relative error in the initial stage implies that the accuracy of the acceleration scheme decreases for a forcing of shorter time scales. For example, at year 500 and 200, the relative errors are about twice and five times that at year 1000. This implies that for a forcing of periods of 500 and 200 years, the relative error of the 6X simulation increases by about 2 and 5 times, respectively, compared with the case of the forcing of the period 1000 years in Figs. 1 and 2.

The time dependency of the acceleration scheme is seen more explicitly in Fig. 3 for experiments of different forcing time scales and acceleration factors. Fig. 3a shows five vertical profiles of the final relative errors for a linear forcing of 1000 years with the acceleration factors of 2, 4, 6, 8 and 10. As expected, an increase of the acceleration factor increases the relative error. This leads to a maximum relative error of about 24% and a volume averaged relative error about 15% in the 10X run. However, it is also seen that the relative error is reduced almost linearly with the increase of the forcing time. For example, the relative error for the 10X run (Fig. 3a) is reduced by almost five times when the forcing period is increased to 5000-year (Fig. 3b), but is almost doubled when the forcing time is reduced to 500-years (Fig. 3c). Similar relationships can be found for other acceleration factors. This nearly linear dependence of the relative error with the time scale of the forcing is consistent with implication from the evolution of the relative error of a single transient simulation as discussed in Fig. 1 and Fig. 2 earlier. Practically, the reduction of the error with the forcing time is an important feature of our scheme, because it is precisely such very long simulations that are beyond our current computational capability and thus most in need of such a scheme. It should be pointed out that even through the conclusion is derived from the cases of linearly increasing forcing, it should also apply to cases

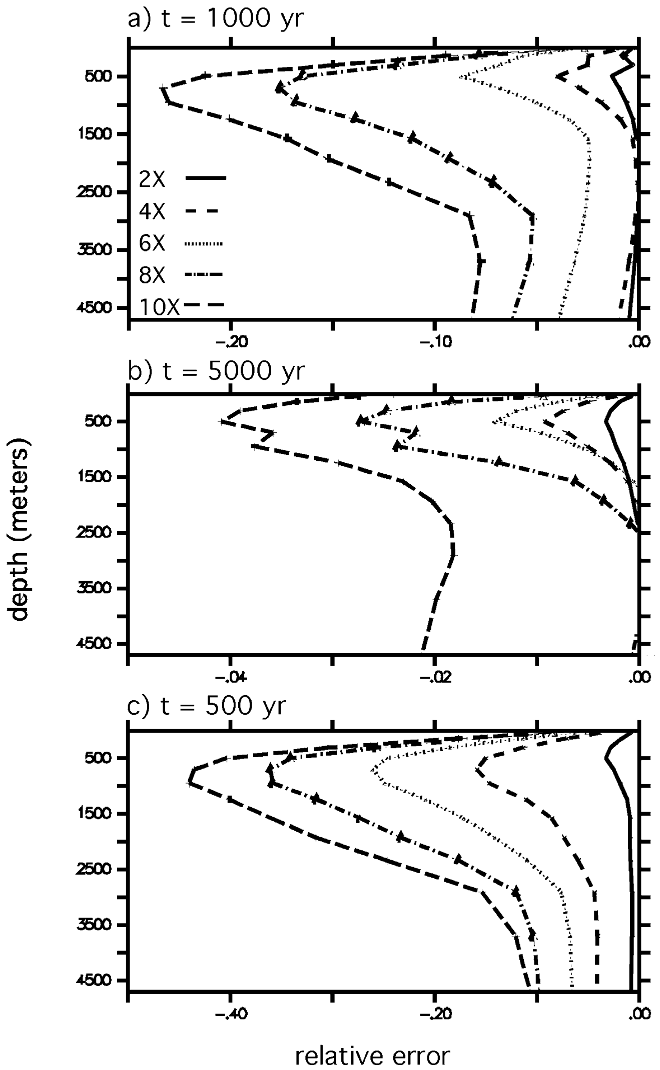

Fig. 3a–c Sensitivity of the relative error to forcing times and acceleration factors. An anomalous global SST forcing is applied that increases linearly to 2 °C in **a** 1000 years, **b** 5000 years and **c** 500 years for each respective 1X run. In *each panel*, the vertical distribution of the final global mean temperature relative errors are plotted for five accelerated runs: 2X, 4X, 6X, 8X and 10X runs. All acceleration runs have the ocean acceleration vertical profile *B* in Fig. 3b. The 6X run has been discussed in details in Figs. 1 and 2

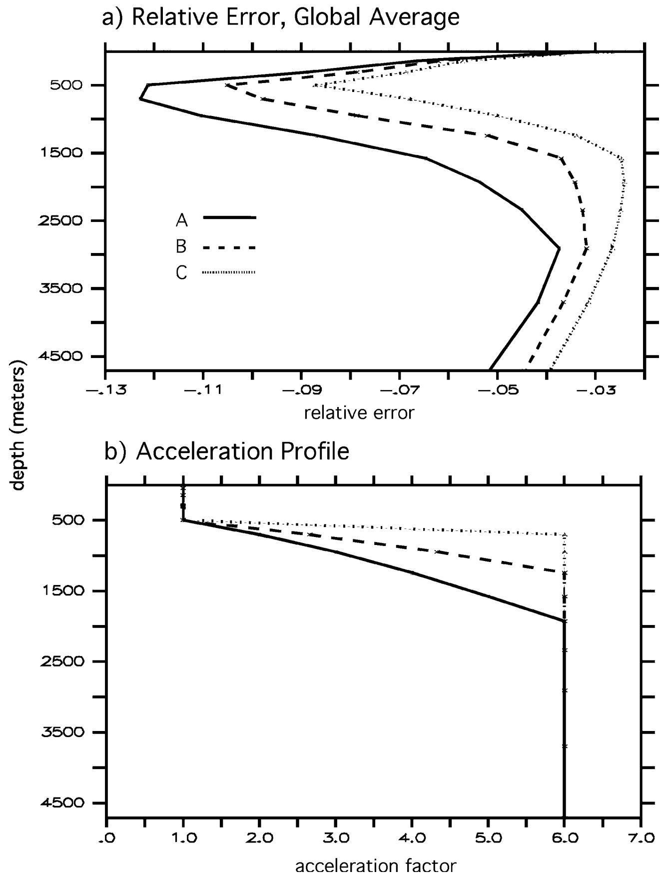

Fig. 4a,b Sensitivity of the relative error to the vertical profiles of ocean acceleration. **a** Vertical distributions of the final global mean temperature relative errors for three 6X simulations that are forced by the same surface forcing as in Figs. 1 and 2, but with different ocean acceleration vertical profiles as shown in **b**. The profile *B* is the standard profile that has been used in other OGCM acceleration simulations. *Each mark* represents the center depth of a model grid. (The 15 levels of the model extend to the depth of 6000 m, of which the lowest two levels are not shown because they only represent a very small region of the ocean)

of periodic forcing with comparable time scales, at least for quasi-linear response to not too strong a forcing. For example, the relative error of a periodic forcing with a 1000-year period should be comparable with that at year 1000 of a simulation under a linearly increasing forcing of duration of 1000 years (or longer). This has been confirmed in our zero-dimension energy balance model (not shown).

3.3 Dependence of the vertical profile of acceleration

The accuracy of the acceleration scheme also depends on the vertical distribution of the acceleration factor. Given a forcing acceleration factor *C*, the shallower the zone of full acceleration (of acceleration factor *C*) extends from the deep ocean, the more closely the partial acceleration scheme resembles the complete acceleration scheme Eq. (4), and therefore the more accurate the partial acceleration scheme should be. This is confirmed by sensitivity experiments of three ocean acceleration profiles (Fig. 4b) that all have an acceleration factor of 6 for the surface forcing and abyssal ocean. The final global mean relative errors are shown as a function of depth for each run (Fig. 4a). Profile *B* is the standard one used previously in Figs. 1, 2 and 3, whose global mean relative error is derived from the final time of Fig. 1c. Profiles *A* and *C* differ from profile *B* in that the full acceleration zone in the deep ocean is extended upward and reduced downward, respectively. As expected, the final relative error is reduced for profile *A*, but increased for profile *C*, significantly.

There is, however, a limitation for improving the accuracy of the acceleration scheme by extending the full acceleration zone upward. For a given time step, the shallower depth the full acceleration zone extends to, the more likely the numerical scheme violates stability criterion. In our examples here, a further shallowing of the full acceleration zone than that in profile *A* leads to numerical instability. Therefore, the choice of the optimal ocean acceleration profile needs to be tested for a particular model configuration and forcing acceleration factor. An optimal ocean acceleration profile is determined by a compromise between a deeper no acceleration zone in the upper ocean and a shallower extension of the full acceleration zone from the deep ocean: the former ensures numerical stability while the latter enhances the accuracy of the acceleration scheme.

There is an additional practical consideration that contraindicates extending the deep ocean full acceleration zone too close to the surface: a less shallow full acceleration zone in the deep ocean should favor a better simulation of internal climate variability. Ocean dynamics is distorted less in the upper ocean if the full acceleration zone stays deeper. Most internal coupled climate variability of interannual to interdecadal time scales depends on ocean dynamics mainly in the upper ocean, such as ENSO (Philander 1990), the Pacific decadal variability (Latif and Barnett 1994; Gu and Philander 1997), the North Atlantic Oscillation (Delworth 1996) and the tropical Atlantic decadal variability (Chang et al. 1997). A sufficiently deep no acceleration zone may enable us to simulate not only the forced slow evolution of the background climate, but also its slow modulation of interannual to decadal climate variability. A full evaluation of this topic,

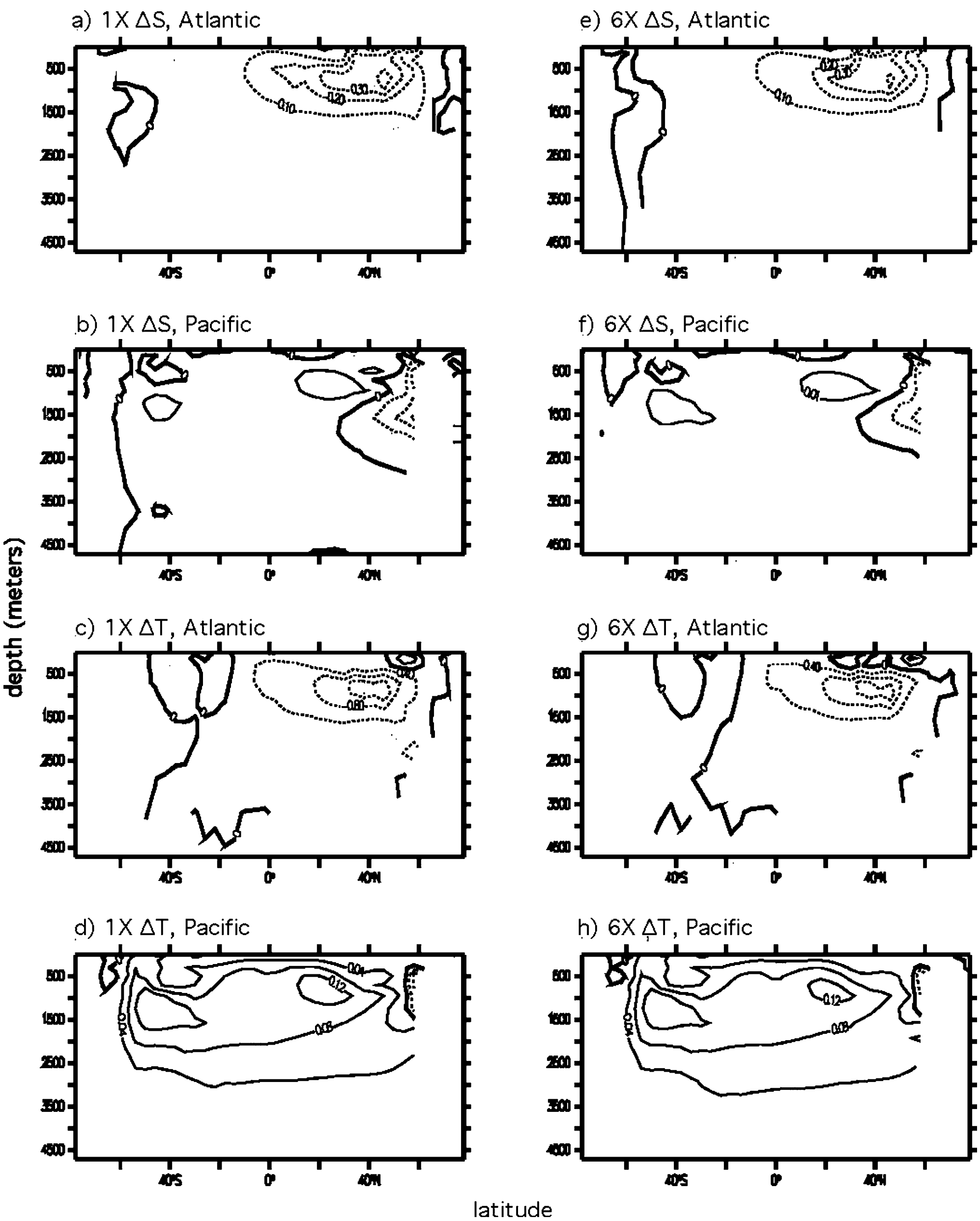

Fig. 5a–h Final basin wide zonal mean salinity and temperature changes forced by a local salinity forcing over the North Atlantic region. The changes in the 1X experiment is shown in **a** Atlantic and **b** Pacific for salinity, and **c** Atlantic and **d** Pacific for temperature. The panels **e**, **f**, **g** and **h** are the same as **a**, **b**, **c** and **d**, respectively, except for being the 6X run. In the 1X run, the anomalous salinity forcing is applied to the restoring SSS over the North Atlantic north of 30°N with a magnitude increasing from 0 ppt at year 0 to –0.5 ppt at year 1000

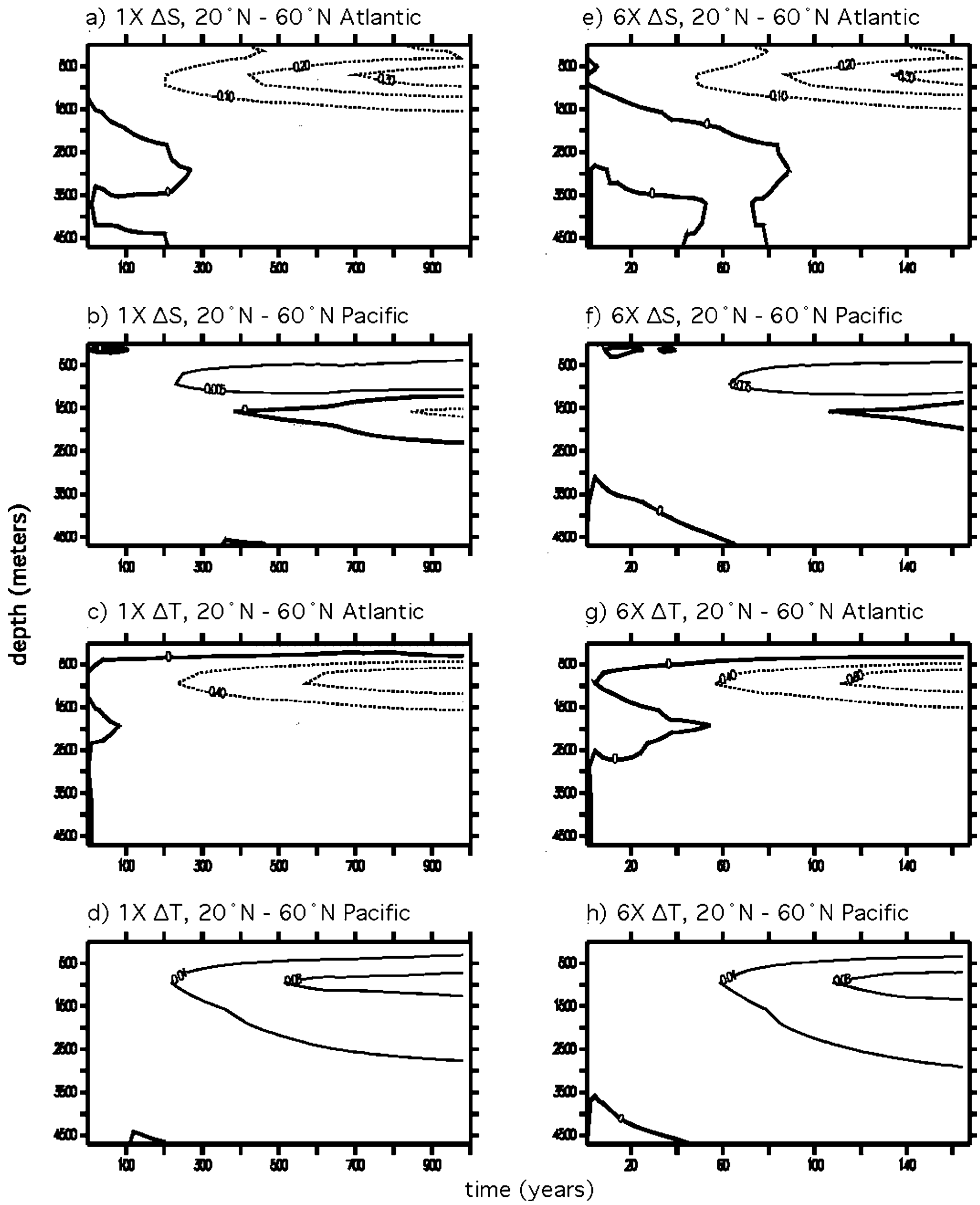

Fig. 6 Evolution of temperature and salinity averaged in 20°N–60°N for the North Atlantic salinity forcing case discussed in Fig. 5 **a**–**d** for the 1X run, and **e**–**h** for the 6X run

however, is beyond our scope because it requires an OAGCM.

3.4 Regional forcing

Our results of the coordinated acceleration scheme above also apply to the cases of regional forcing. Figure 5 and Figure 6 show an example that is forced by a localized salinity forcing in the North Atlantic (>30°N), where the restoring salinity anomaly is increased linearly to 0.5 ppt in 1000 years. Two parallel runs (1X and 6X) are performed with the ocean acceleration profile *B* in Fig. 4b. For the synchronous coupled 1X run, the final zonal mean salinity changes are shown in Figs. 5a,b for the Atlantic and Pacific, respectively; the final zonal mean temperature changes are shown in Figs. 5c,d for the Atlantic and Pacific, respectively. The corresponding changes for the 6X run at the final year (year 166) are shown in Fig. 5e–h. A comparison of the two runs shows a striking overall similarity in all the plots. Similar correspondence of the 1X and 6X can also be found in the time evolution of the temperature and salinity anomalies for selected regions (Fig. 6a–d versus Fig. 6e–h). Overall, the 6X run captures all the major features of the 1X run, but with a slightly delayed response as in the cases of the globally uniform forcing discussed before.

3.5 Dependence on surface boundary condition

The OGCM simulations discussed have used a restoring surface boundary condition, with a 30-day restoring time. This surface boundary condition also affects the accuracy of the accelerated OGCM simulations: a shorter restoring time tends to give a better accelerated simulation, most obviously near the surface. This artificial dependence on the restoring time will not exist in a coupled OAGCM, where the SST response to climate forcing is determined internally by ocean-atmosphere interactions. The short restoring time of 30 days here may be proper for local SST anomalies of sub-basin scales, but may be too strong a damping for basin scale SST anomalies. The latter tends to be damped primarily by longwave radiation, with an equivalent damping time up to about 200 days (for a 30-m or so mixed layer here, Bretherton 1982). With this long restoring time, the acceleration scheme should become less accurate. It is therefore conceivable that our acceleration scheme may become less accurate in a coupled model than as discussed in our OGCM. As a preliminary assessment of the effect of ocean-atmosphere coupling on the acceleration scheme, we repeat the 6X OGCM experiment in Fig. 1 but with the surface restoring time increased about 7 times to 200 days. The result shows an evolution of the vertical profile of the global mean relative error similar to that of the 30-day restoring case in Fig. 1, except for a magnitude about twice larger (not shown). For example, the final maximum relative error still occurs at the depth of 500-m, but reaches about 15%. This experiment implies that the coupling may deteriorate the performance of the acceleration scheme, but not too significantly.

4 Application to a coupled climate model of intermediate complexicity

As a further test of the effect of ocean-atmosphere coupling on the coordinate acceleration scheme, we applied the coordinated acceleration scheme to a coupled climate model of intermediate complexity CLIMBER-2 (Petoukhov et al. 2000). CLIMBER-2 has been shown to be similar to OAGCMs in respect to an equilibrium and transient response to different climatological forcings (Ganopolski et al. 2001) and mimics many aspects of an OAGCM. At the same time CLIMBER-2 is up to four orders of magnitude faster than a normal OAGCM, which allows us to perform in a short time a large set of long-term simulations.

We implemented in the ocean component of the CLIMBER-2 model the same acceleration scheme as described for the OGCM in the last section. We first compare the accelerated control runs (with no anomalous climate forcing) with the synchronously coupled control run (1X, standard CLIMBER-2). It is found that the acceleration affects the mean climate state, but only slightly. The final global surface air temperatures at year 1000 are warmer than the synchronously coupled control run by 0.1, 0.2 and 0.3 °C, for 2X, 4X and 6X acceleration, respectively. These values are small, and we have tested that the acceleration has negligible impact on model sensitivity to different climate forcings. The reason for the distortion of the climate in the equilibrium control run is that the acceleration is not applied to the procedure of convective adjustment. Thus, even in an equilibrium climate run, deep ocean acceleration no longer conserves energy completely. The impact of the acceleration scheme is larger at high latitudes where deep convection occurs. The accelerated model in general tends to be slightly warmer, primarily due to a reduction of the ice cover. A similar climate drift has been noted in other acceleration schemes (Voss and Sausen 1996). Although the causes of the drift differ among different methods, they tend all to be related to the nonlinearity of the coupled system.

This small model biases introduced by the acceleration in CLIMBER-2, we speculate, should be reduced in a 3-D OAGCM. This follows because CLIMBER-2 is based on the multi-basin zonally averaged ocean model. In such an ocean model the volume of the ocean involved in each deep convection event is unrealistically large since any deep convection event occurs in the entire longitudinal circle of the ocean basin. In reality, or in a 3-D OGCM, a deep convection event tends to be confined in a small area in both the zonal and meridional directions. Indeed, similar acceleration control simulations performed in our 3-D OGCM produce little climate drift. The largest drift of global mean ocean temperature at the end of 1000-year is less than 0.01 °C even for an acceleration factor of 10. This leads us to speculate that the magnitude of the climate drift derived from CLIMBER-2 may represent an upper bound of the distortion of climate state due to the acceleration. This speculation needs to be confirmed in an OAGCM.

To assess the performance of acceleration in transient runs, we performed a set of experiments with exponentially growing atmospheric CO_2 concentration, which implies an approximately linearly-increasing radiative forcing. The rate of CO_2 increase is selected to produce a global average SST change similar to the noted OGCM experiments: about 2 °C in 1000 years in the standard 1X experiment. In the experiments with the acceleration factor C, the rate of CO_2 growth is enhanced by the same factor C while the length of the model run is decreased compared to the standard run by the same factor. Even through the small drift has little effect on the CLIMBER-2 experiments, we still chose to completely exclude this drift for our transient sensitivity experiments later. For each acceleration factor, an individual spin-up run was performed to achieve an exact equilibrium state before the anomalous climate forcing is applied. (The integration time to reach the spin-up equilibrium is considerably shorter for the acceleration experiment than for the standard synchronously coupled experiment, by a factor approximately inversely proportional to the acceleration factor).

Figure 7a shows that even for the 6X run changes of global mean surface air temperature at the end of the run are within 10% of the true experiment. The same is true for the globally averaged SST (not shown). The

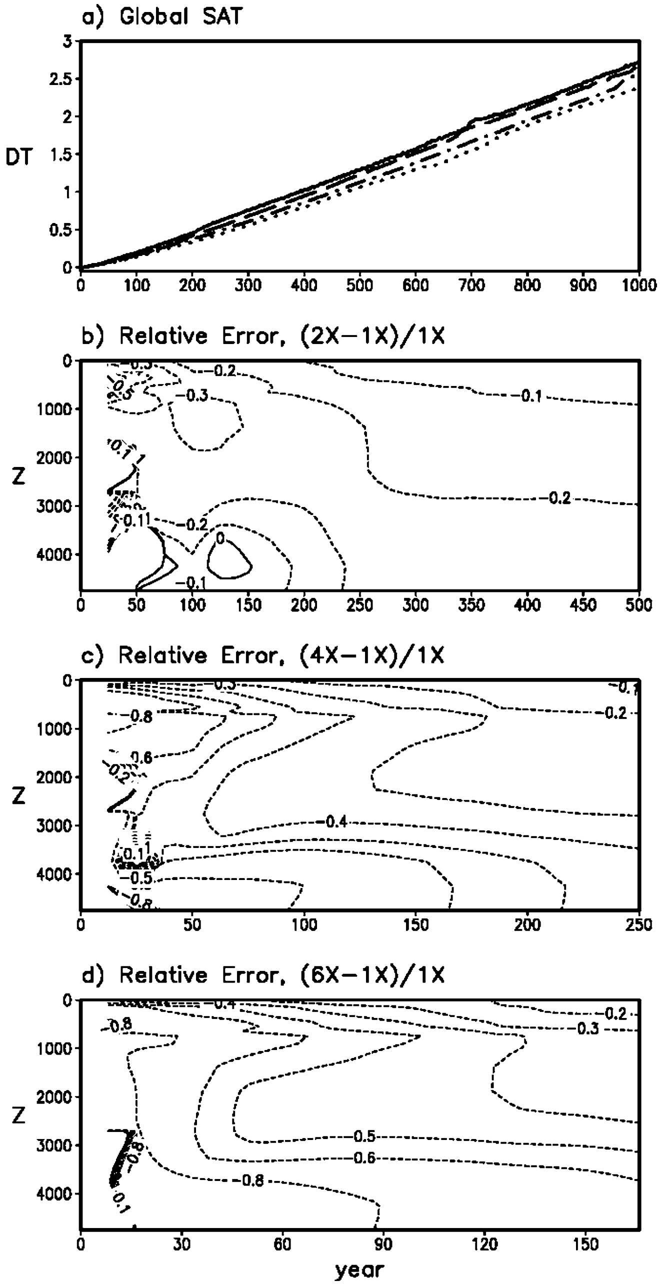

Fig. 7 CLIMBER-2 model simulations for **a** evolution of global mean annual surface air temperature in response to an exponential growth of CO_2 concentration in 1X (*solid*), 2X (*dashed line*), 4X (*dashed-dotted line*) and 6X (*dotted line*) experiments. The vertical profile of relative error of the global mean ocean temperature is shown in the **b** 2X, **c** 4X and **d** 6X experiments. The vertical profile of the ocean acceleration is similar to the profile B in Fig. 3b

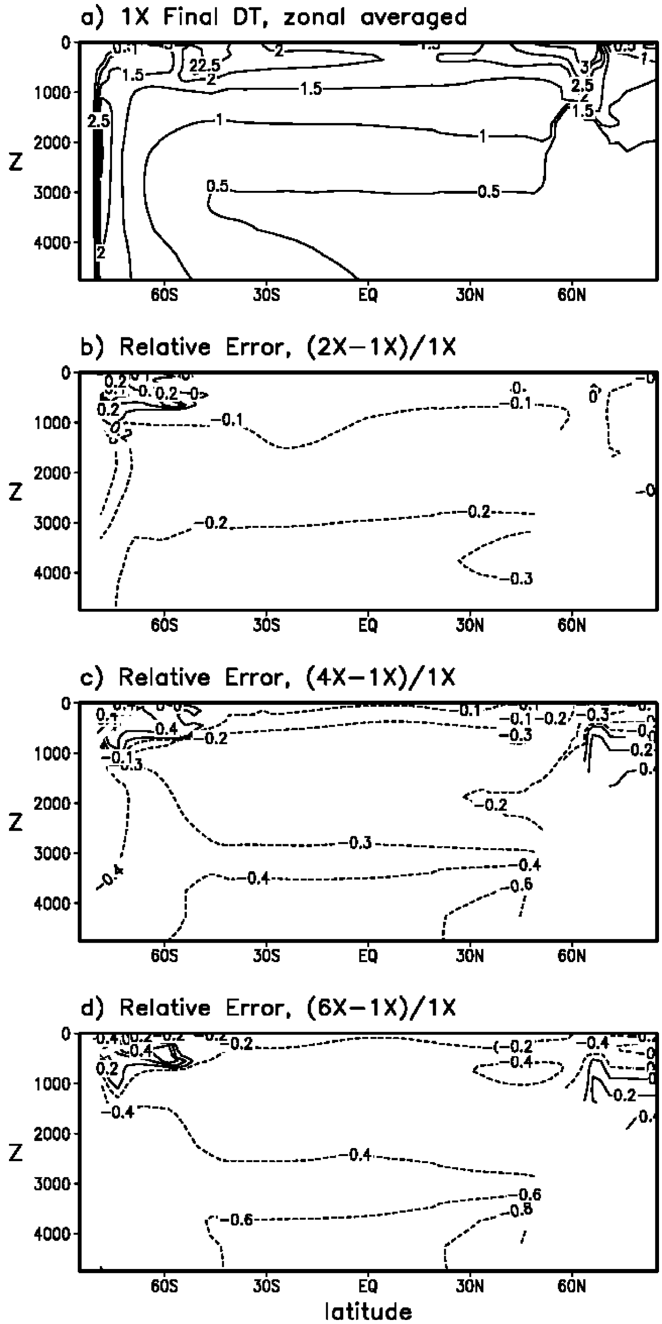

Fig. 8 CLIMBER-2 model results. Meridional section of the final zonal mean global ocean temperature for **a** the absolute temperature changes of the 1X experiment, and relative temperature errors in accelerated **b** 2X, **c** 4X and **d** 6X experiments at the end of each experiment

relative temperature errors in the ocean (Figs. 7b,c, or 8b,c) are dominantly negative, as in the OGCM case. Except in the case of 2X, the relative error also tends to reach a local maximum at intermediate depths between 500 and 1000-m, also similar to the OGCM case. However, as expected, relative errors are larger in CLIMBER-2 than in the OGCM. At the end of the 1000-years, the magnitude of relative errors are about 0.1, 0.2, 0.3 in the upper ocean for the experiments of 2X, 4X and 6X, respectively. This is about two (four) times that of the OGCM experiments with a 200-day (30-day) surface restoring time. Somewhat unexpectedly, the relative error in all CLIMBER-2 accelerated experiments tends to reach the maximum in the bottom ocean. This is opposite to the OGCM experiments, in which the relative error tends to decrease towards the abyss (Figs. 1–6). As a result, the relative error in the deep ocean is substantially larger in CLIMBER-2 than in the

OGCM. This large relative error in the deep ocean appears to be associated mainly with deep convections at high latitudes, especially in the Southern Ocean (Fig. 8). The large relative error may be amplified by the sea-ice albedo feedback. It may also be amplified by the exaggerated role of convective events in the 2-D ocean model of CLIMBER-2, as discussed earlier regarding the climate drift in the accelerated control run. In addition, this large relative error may also be caused by the underestimated circulation time of the bottom water in the 2-D ocean in CLIMBER-2; its 2-D ocean circulation lacks horizontal gyre circulation routes which are the dominant circulation routes for a 3-D ocean circulation. Since the idea of the coordinated acceleration is based physically on the time scale separation, between the long deep ocean circulation time and the shorter upper ocean circulation time, a shorter circulation time of the deep ocean tends to narrow down this time scale separation and therefore contributes to an increased error in the deep ocean. Based on the discussions above, we speculate that the relative error in an OAGCM will be smaller than that in CLIMBER-2, especially in the deep ocean. This speculation, however, needs to be confirmed with an OAGCM.

These relative temperature errors correspond to small absolute temperature changes and have relatively little effect on other climate variables, such as the North Atlantic overturning circulation, global salinity and sea-ice cover. These climate variables all show reasonable agreement with the standard experiments. For example, the reduction of the North Atlantic overturning circulations (not shown) are almost the same (8 Sv) in the 2X, 4X and 6X experiments as in the 1X experiment.

5 Conclusions and discussion

A new acceleration scheme is proposed for the simulation of long climate evolutions in a coupled ocean-atmosphere model. In this coordinated acceleration scheme, both the surface forcing and deep ocean are accelerated simultaneously by the same factor. The acceleration scheme is evaluated first in a 3-D OGCM and then in a coupled ocean-atmosphere model of intermediate complexity. For millennial climate evolution, the acceleration scheme is found to produce reasonable results with an acceleration of about five times. For even longer climate evolution, the acceleration factor can be improved further.

Earlier acceleration schemes for a coupled model are designed to reduce the computation time of the atmospheric component model only (Manabe and Bryan 1969; Schlesinger 1979; Sausen and Voss 1996; Voss et al. 1998; Liu et al. 1999). The general deep water acceleration scheme of Bryan (1984) does reduce the ocean computation time, but it only applies to equilibrium climate simulations. Our coordinated acceleration scheme achieves both: it reduces oceanic computation time as much as the atmospheric computation time and it is also effective for (long-term) transient simulations. However, the coordinated acceleration scheme has one major limitation: it applies only to climate evolution forced by an external forcing of very long time scales, millennial or even longer. These simulations are usually of paleoclimate applications. One important feature of the coordinate acceleration is that the longer the evolution, the better the acceleration scheme. Practically, this is a very useful feature because it is precisely those very long simulations that require the acceleration the most.

We speculate that the coordinated acceleration scheme will not distort short-term climate variability substantially, including the annual cycle, interannual (such as ENSO) and decadal (such as PDO) variability. This is based on the physical mechanisms of the variability. Interannual to decadal variability involves mainly ocean dynamics in the upper ocean (less than 1000-m in the thermocline). The annual cycle signal is mostly confined within the surface mixed layer (except at very high latitudes where deep convection penetrates into the deep ocean) (Note that both the OGCM and CLIMBER-2 experiments discussed have the full seasonal cycle in their mean state. The acceleration of the forcing is applied only to the anomalous forcing). Therefore, our acceleration scheme could also be useful for studying the modulation effect of a slow evolving mean climate on short-term internal variability. Our scheme is most likely to underestimate climate variability at centennial time scales, because of the potential involvement of deep ocean and thermohaline circulation. This scale is likely to be the worst time scale for our scheme because it is between the interannual upper ocean time scale and the millennial slow evolution time scale, and because it is comparable with the time scale of the intermediate water which tends to be distorted the most in our scheme. All these speculations, however, need to be confirmed with an OAGCM. In comparison, the asynchronous coupling scheme (Manabe and Bryan 1969), we speculate, is problematic for studying short and long internal climate variability. This is because this scheme distorts (or accelerates) the dynamics of the entire ocean, including the surface ocean such that ocean-atmosphere interaction is distorted at shorter time scales. The periodically synchronous coupling has been shown to underestimate short term SST variability but to overestimate longer term SST variability (Voss et al. 1998). This scheme is also somewhat inconvenient for the study of atmospheric variability, because of a discontinuity of the atmospheric simulation between each synchronous coupling period.

In general, no acceleration scheme is perfect for a nonlinear system like a coupled OAGCM. Even for the case of steady forcing (Bryan 1984; Voss and Sausen 1996; Liu et al. 1999), the accelerated system would always converge towards the correct final state only if the original system has a single final equilibrium. The transient simulation here is much more complicated and therefore any acceleration scheme for the transient evolution will induce errors. The practical issue, however, is a balance between computation time and the phenomenon of interest. For the application of the coordinated acceleration scheme, we propose two general principles. The coordinated acceleration is preferred if both principles are satisfied. First, the climate evolution of main interest is forced by an external forcing of a time scale longer than 1000 years. In this case, the acceleration factor can be 3–5, or even higher if the time scale is even longer. The most effective acceleration factor, and vertical profile of the ocean acceleration, however, can only be tested for each model itself. Second, the ocean component of the OAGCM uses a substantial amount of the total computation time. In this case, neither the asynchronous coupling nor the periodically synchronously coupling is able to save the computation time for the ocean.

This study presents the main idea of the coordinated acceleration scheme, but only in simplified models. A full assessment of this scheme, however, requires the application to an OAGCM. This will be performed in the future.

Acknowledgements We would like to thank the two anonymous reviewers, whose comments have helped improving the paper substantially. This is CCR contribution 843.

References

Bretherton FP (1982) Ocean climate modeling. Progress in oceanogaphy Vol 11, Pergamon, Oxford, pp 93–129

Bryan K (1984) Accelerating the convergence to equilibrium of ocean-climate models. J Phys Oceanogr 14: 666–673

Chang P, Ji L, Li H (1997) A decadal climate variation in the tropical Atlantic Ocean from thermodynamic air-sea interactions. Nature 385: 516–518

Delworth T (1996) North Atlantic interannual variability in a coupled ocean-atmosphere model. J Clim 9: 2356–2375

Ganopolski A, Petoukhov V, Rahmstorf S, Brovkin V, Claussen M, Eliseev A, Kubatzki C (2001) CLIMBER-2: a climate system model of intermediate complexity. Part II: model sensitivity. Clim Dyn 17(10): 735–751

Gu D, Philander SGH (1997) Interdecadal climate fluctuations that depend on exchanges between the tropics and extratropics. Science 275: 805–807

Latif M, Barnett TP (1994) Causes of decadal climate variability over the North Pacific and North America. Science 266: 634–637

Liu Z, Gallimore R, Kutzbach J, Xu W, Golubev Y, Behling P, Siegle R (1999) Modeling long term climate change with the equilibrium asynchronous coupling scheme. Clim Dyn 15: 325–340

Luyten J, Pedlosky J, Stommel H (1983) The ventilated thermocline. J Phys Oceanogr 13: 292–309

Manabe S, Bryan K (1969) Climate calculations with a combined ocean-atmosphere model. J Atmos Sci 26: 786–789

Pacanowski RC, Griffies S (1998) MOM 3.0 Manual, NOAA/Geophysical Fluid Dynamics Laboratory, Princeton, USA 08542

Petoukhov V, Ganopolski A, Brovkin V, Claussen M, Eliseev A, Kubatzki C, Rahmstorf S (2000) CLIMBER-2: a climate system model of intermediate complexity. Part I: model description and performance for present climate. Clim Dyn 16(1): 1–17

Philander SGH (1990) El Nino, La Nina, and the Southern Oscillation. Academic Press, San Diego, USA

Sausen R, Voss R (1996) Techniques for asynchronous and periodically-synchronous coupling of atmosphere and ocean models. Part I: general strategy and application to the cyclostationary case. Clim Dyn 12: 313–323

Schlesinger ME (1979) Discussion of "A global ocean-atmosphere model with seasonal variation for future studies of climate sensitivity". Dyn Atmos Oceans 3: 427–432

Voss R, Sausen R (1996) Techniques for asynchronous and periodically-synchronous coupling of atmosphere and ocean models. Part I: impact of variability. Clim Dyn 12: 605–614

Voss R, Sausen R, Cubasch U (1998) Periodically synchronously coupled integrations with the atmosphere-ocean general circulation model ECHAM3/LSG. Clim Dyn 14: 249–266